



# Unveiling obscured accretion

F. Fiore

Istituto Nazionale di Astrofisica – Osservatorio Astronomico di Roma, via Frascati 33 I-00040 Monteporzio, Italy e-mail: [fiore@mporzio.astro.it](mailto:fiore@mporzio.astro.it)

**Abstract.** We present the latest determination of the X-ray (2-10 keV) AGN luminosity function accounting for the selection effect due to X-ray absorption. The main results are: 1) the inclusion of obscured AGN confirms the AGN differential luminosity evolution, but makes it less extreme than what is found selecting unobscured AGN in soft X-rays, and more similar to a pure luminosity evolution; 2) significant correlations are found between the fraction of obscured sources, the luminosity and the redshift, this fraction increasing toward both low AGN luminosities and high redshifts. We discuss our findings in a scenario for the formation and evolution of the structure in the Universe where the bulk of nuclear activity is produced at  $z \sim 1 - 2$ . At the same redshifts also the star-formation rate reaches a maximum, and this age can therefore be regarded as the "golden age" for nuclear and galaxy activity. We discuss the current observational limits of this program and the improvements needed to obtain an unbiased census of the AGN and super-massive black hole (SMBH) population.

## 1. Introduction

Active Galactic Nuclei are not only witnesses of the phases of galaxy formation and/or assembly, but most likely among the leading actors. Indeed, two seminal discoveries indicate tight links and feedbacks between SMBH, nuclear activity and galaxy evolution. The first is the discovery of SMBH at the center of most nearby bulge dominated galaxies, and, in particular, the steep and tight correlation between their masses and galaxy bulge properties (see e.g. Ferrarese & Merrit 2000, Gebhardt et al. 2000, Marconi & Hunt 2003). The second discovery was originally due to the first deep X-ray surveys performed by ROSAT at the beginning of the 90'. They showed that the evolution of AGN is luminosity dependent. On average, the activity of Seyfert like objects rises up to  $z \approx$

1 and then decreases, while QSO activity rises smoothly up to  $z=2-3$  or even further (Miyaji et al. 2000 and references therein). The former recalls the evolution of star-forming galaxies, while the latter recalls the evolution of massive spheroids (Franceschini et al. 1999). However, soft X-ray surveys are biased against obscured sources, which, on the other hand, are very common in the local Universe. Indeed, the first imaging surveys above 2 keV obtained with ASCA and BeppoSAX found the first sizeable samples of highly obscured AGN at  $z > 0.1$  and confirm, at least qualitatively, the predictions of standard AGN synthesis models for the Cosmic X-ray Background, CXB (Fiore et al. 1999, Akiyama et al. 2000, La Franca et al. 2002, Ueda et al. 2003). Chandra and XMM-Newton surveys confirm and expand this picture. On one side they resolved nearly 100% of the CXB below 2 keV (Giacconi et

---

Send offprint requests to: F. Fiore

al. 2002, Brandt et al. 2001) and confirm the strong luminosity dependent density evolution of soft X-ray sources (Hasinger 2003, 2005). On the other side deep and large area surveys up to 10 keV clearly showed that AGN activity spans a range of optical to near-infrared properties much greater than it was thought based on optically and soft X-ray selected AGNs (Fiore et al. 2003, Koekemoer et al. 2004, Barger et al. 2005). The main reason is that hard X-ray selection provides a more complete and direct view of AGN activity, being less biased than optical or soft X-ray selection against obscured sources. For example, 2-10 keV surveys pick up AGN relatively bright in X-rays but with extremely faint optical counterparts. The majority of these sources have been identified as highly obscured, high luminosity AGN at  $z \gtrsim 1$ , the so called type 2 QSOs ( $\sim 20$  in the HELLAS2XMM survey, 3/4 confirmed through optical spectroscopy, Fiore et al. 2003, Mignoli et al. 2004, Maiolino et al. 2006, Cocchia et al. 2006, about 30 in the CDFS+CDFN, half of which confirmed through optical spectroscopy; a dozen in the CLASXS survey, Barger et al. 2005). At the opposite of the X-ray to optical flux ratio distribution, Chandra and XMM-Newton hard X-ray surveys discovered moderately obscured sources with AGN luminosity, in otherwise inactive, optically bright, early type galaxies (named X-ray bright, optically normal galaxies, XBONGs, Fiore et al. 2000, Comastri et al. 2002).

In this paper we discuss how the inclusion of obscured AGN affects the determination of the AGN luminosity function, and discuss our findings in the framework of semi-analytical models for the formation and evolution of the structure in the Universe.

## 2. The evolution of hard X-ray selected sources

Figure 1 gives an overview of the flux limits and surveyed areas of major AGN surveys carried out over the last years in the 2-10 keV band. In this paper we use the source samples given in Table 1, which include the deepest surveys performed with Chandra as well as larger

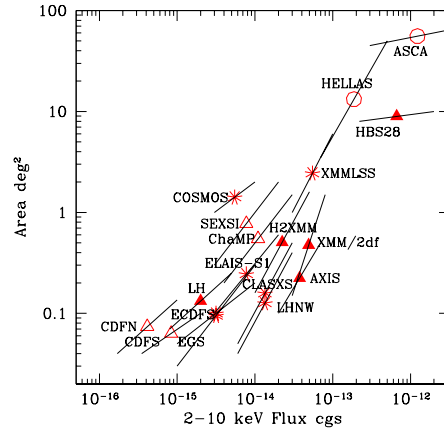


**Fig. 1.** Solid angles and flux limits of AGN surveys carried out in the 2-10 keV band. Triangles represent serendipitous surveys constructed from a collection of pointed observations (Chandra open symbols; XMM-Newton filled symbols; BeppoSAX and ASCA surveys are also reported). The asterisks represent surveys covering contiguous areas.

area surveys performed with XMM-Newton and ASCA, plus the so-called Piccinotti sample of local AGN.

We estimated the 2–10 keV luminosity function by fitting the expected number of AGN in bins of luminosity, redshift and rest frame absorbing column density  $N_H$  (La Franca et al. 2005). This allows us to take into account observational selection effects. In particular, we correct for the selection effect due to X-ray absorption, and for the incompleteness of the optical spectroscopy identification (see La Franca et al. 2005 for details). Our results extend those of Fiore et al. (2003), Cowie et al. 2003 and Barger et al. (2005). In all these three papers no correction for the X-ray absorption is adopted. Fiore et al. (2003) assign a redshift to the sources without spectroscopic identification using statistical arguments; Cowie et al. (2003) and Barger et al. (2005) estimate upper limits to the AGN density by assigning to the unidentified sources the redshifts corresponding to the centers of each  $L_X$ - $z$  bin.

Figure 2 and 3 show the best fit  $N_H$  distribution and best fit luminosity functions

**Table 1. 2-10 keV surveys**

Sample	Tot. Area deg <sup>2</sup>	Flux limit 10 <sup>-15</sup> cgs	# sour.	% z-spec
HELLAS2XMM	1.4	6.0	232	70%
CDFN faint <sup>a</sup>	0.0369	1.0	95	59%
CDFN bright <sup>b</sup>	0.0504	3.0	51	65%
CDFS faint <sup>a</sup>	0.0369	1.0	75	62%
CDFS bright <sup>b</sup>	0.0504	3.0	52	60%
Lockman Hole <sup>c</sup>	0.126	2.6	55	75%
HBS28	9.8	22	28	100%
AMSSn	69	30	74	100%
Total			662	75%

<sup>a</sup> Inner 6.5 arcmin radius; <sup>b</sup> outer 6.5–10 arcmin annulus; <sup>c</sup> inner 12 arcmin radius; <sup>d</sup> inner 4.5 arcmin radius. See La Franca et al. 2005 for details.

for a luminosity-dependent density evolution (LDDE) model (La Franca et al. 2005, see also Miyaji et al. 2000 for a similar parameterization). The parameters of the evolving luminosity function and of the dependencies of the  $N_H$  distribution by  $L(2-10 \text{ keV})$  and  $z$  have been fitted simultaneously. The intrinsic  $N_H$  distribution (dotted lines in figure 2) is flat above  $10^{21} \text{ cm}^{-2}$ , while the fraction of objects with  $N_H < 10^{21} \text{ cm}^{-2}$  is one of the model parameters. The dashed lines show the predictions when the selection effects due to X-ray absorption, which pushes sources below the X-ray detection limit, and to the incompleteness of the spectroscopic identification are taken into account. As expected, most AGN with  $N_H > 10^{24} \text{ cm}^{-2}$  are lost in even the deepest Chandra and XMM 2-10 keV surveys. In addition, note that about 2/3 of the AGN with  $10^{23} < N_H < 10^{24} \text{ cm}^{-2}$  are also lost at  $z < 1$ . Our best fit luminosity function recovers all these highly X-ray obscured AGN, as well as optically obscured AGN, whose optical counterpart is too faint to allow a spectroscopic identification.

The best fit 2-10 keV luminosity function is compared to the best fit 0.5-2 keV total luminosity function of Miyaji et al. (2000) and to the best fit 0.5-2 keV type 1 AGN luminosity function of Hasinger et al. (2005) in figure 3. These functions falls shorter than the 2-10 keV luminosity function by a factor 3-10 at luminosities  $\log L_X = 42.5 - 43$  in the three lowest redshift bins. (At  $z > 1.5$  the comparison is less informative because the present 2-

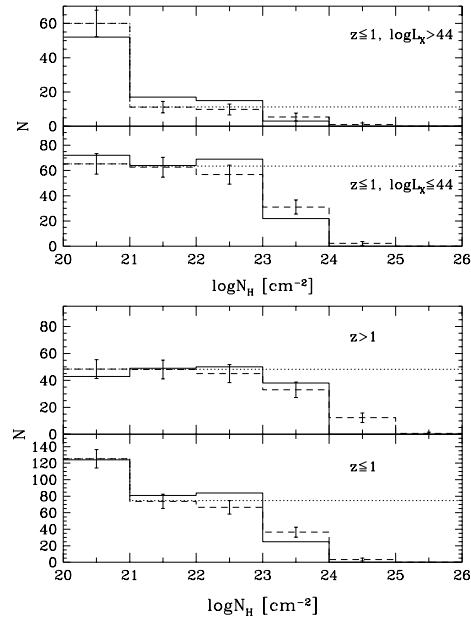


**Fig. 2.**  $N_H$  distributions in four luminosity and redshift bins. The dotted lines are the assumed  $N_H$  distributions, the dashed lines are the expectations taking into account the selection effects and the continuous lines are the observed distributions.

10 keV data do not go deep enough to provide samples of low luminosity AGNs large enough to constrain adequately their space density.) Conversely, a better agreement between the 0.5-2 keV and the 2-10 keV luminosity functions is found at the highest luminosities sam-

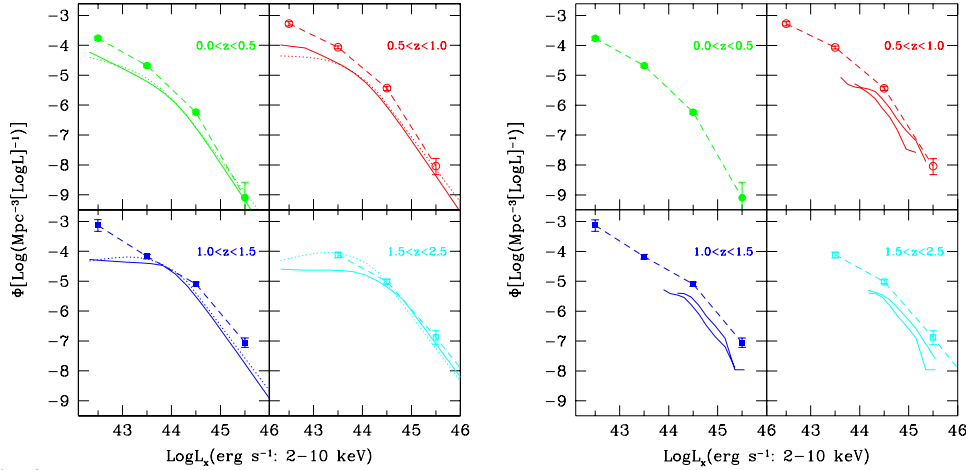


**Fig. 3.** The 2-10 keV luminosity function in four redshift bin, compared to the 0.5-2 keV luminosity function of Miyaji et al (2000, left panel, dotted lines), with the 0.5-2 keV type 1 AGN luminosity function of Hasinger et al. (2005, left panel, solid lines) and with the optical (B band) luminosity function of Croom et al. (2004, right panel). Two optical luminosity function are plotted in each quadrant, corresponding to redshift bridging the range used for the 2-10 keV luminosity function. The conversion factor to pass from the 0.5-2 keV to the 2-10 keV band has been calculated assuming a power law spectrum with  $\alpha = 0.8$  while that to pass from the B band to the 2-10 keV band has been computed following Marconi et al. 2004.

pled, with the exception of the  $z=1-1.5$  bin. Hasinger et al. (2005) exclude from their analysis X-ray (and/or) optically obscured AGN, which in any case are not an important population in 0.5-2 keV surveys. Indeed the Hasinger et al. luminosity function is nearly identical to the Miyaji et al. (2000) one at least at  $z < 1.5$ . (At  $z > 1.5$  the Miyaji et al. 2000 best fit overpredicts the number of low luminosity AGN, probably because to the larger uncertainties at high redshift and low luminosity due to the much shallower data used in comparison with Hasinger et al. 2005). Obscured AGNs are recovered in the 2-10 keV luminosity function. The result is that the evolution of this luminosity function deviates less from a pure luminosity evolution than the soft X-ray luminosity functions. At least part of the strong luminosity dependent density evolution claimed based on the 0.5-2 keV data is therefore due to the exclusion of obscured AGN.

Figure 3 compares the 2-10 keV and optical luminosity functions. Luminosity dependent conversion factors to pass from the B band to the 2-10 keV band have been computed

following Marconi et al. (2004). It should be borne in mind that the uncertainty on the conversion factor may be as large as a factor of two. Note that the low luminosity end of the optical luminosity function is always 1, 1.5 dex higher than that of the X-ray luminosity function. This is due to the difficulty in selecting low luminosity AGNs against their host galaxy in the optical band. The optical luminosity function is similar or slightly lower than the 0.5-2 keV luminosity function at  $z > 0.5$ , and therefore the same comments given above for the soft X-ray luminosity function apply also in this case: e.g. a large fraction of obscured accretion may be missed by both optical and soft X-ray selection.

Figure 4 shows the fraction of X-ray obscured AGN ( $N_H > 10^{22} \text{ cm}^{-2}$ ) as a function of the 2-10 keV luminosity and the redshift. The long dashed lines are the best fit intrinsic distributions while the short dashed lines are the expectations taking into account all selection effects described above. Both the observed and best fit fraction of obscured AGN at  $z < 1$  decrease strongly with the AGN lumi-

luminosity, a behavior already noticed in the literature since the first Einstein systematic observations of QSO (Lawrence & Elvis 1982), and confirmed quantitatively by Ueda et al. (2003). Note that this trend becomes more evident putting together deep surveys, well sampling low luminosity AGN, and large area surveys, which can provide large samples of luminous AGN. Note also that selection effects affects in a similar way low and high luminosity AGN: the ratio of the intrinsic and predicted fractions of obscured AGN is nearly constant with the luminosity. This is not the case when considering the dependence of the fraction of obscured AGN with the redshift. The reason is that obscured AGN are much more likely to be missed in X-ray surveys at low redshift than at high redshift, because the photoelectric cut-off is quickly redshifted toward low X-ray energies. Indeed, comparing the best fit intrinsic distribution to the distribution expected after the selection effects, we note that while we loose just about 15% of the obscured AGN at  $z=2$  slightly less than half are lost at  $z < 0.2$ . By correcting for this selection effect we find that the intrinsic fraction of obscured AGN in the luminosity range  $10^{43} - 10^{46}$  still increases by a factor 1.8 from  $z=0$  to  $z=2$ . This new result is due a better coverage of the luminosity-redshift diagram in comparison with previous work.

Figure 5 shows the luminosity-redshift plane for the surveys in Table 1. The arrows indicate the directions in which the fraction of obscured AGN increases, according to figure 4. Excluding the CDFS and CDFN data would strongly limit the number of AGN with  $\log L(2-10) < 44$  (those more likely to be obscured, according to the left panel of figure 4), making difficult to asses any trend with the redshift. The arrows indicate also the direction in which the flux decreases. Indeed a strong correlation of the number of obscured AGN and the flux has been reported in the past (Piconcelli et al. 2003, Ueda et al. 2003, Perola et al. 2004) and it is expected by AGN synthesis models of the CXB (Comastri et al. 2001). Figure 5 shows this correlation for the source sample in Table 1, along with the best fit LDDE model of La Franca et al. (2005). In conclusion, the correlations found between the fraction of obscured

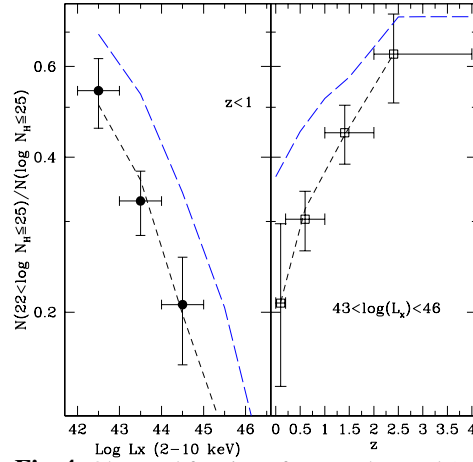


**Fig. 4.** Observed fraction of X-ray obscured ( $N_H > 10^{22} \text{ cm}^{-2}$ ) AGN as a function of  $L(2-10\text{keV})$  and  $z$ . The long dashed lines are the best fit intrinsic distributions. The short dashed lines are the expectations taking into account all selection effects.

AGN and luminosity and redshift of figure 4 confirm and extend previous determinations, based on smaller and shallower surveys.

### 3. Discussion

Our determination of the 2-10 keV AGN luminosity function, accounting for selection effects due to nuclear obscuration by gas and dust, confirms the AGN differential luminosity evolution, but makes it less extreme than what is found selecting unobscured AGN only (see e.g. Hasinger et al. 2005). This is important for both models that make use of the AGN luminosity function (to reproduce the X-ray and IR Cosmic backgrounds for example), and for models which try to explain the AGN luminosity function, as the semi-analytic, hierarchical clustering model proposed by Menci et al. (2004). Figure 6 compares the AGN number density as a function of  $z$  with the predictions of the Menci model. The result is qualitatively similar to that reported by Menci et al. (2004). The trend of lower luminosity AGN peaking and increasingly lower redshift is found in both data and model, which however predicts a number of low-to-intermediate luminosity (Seyfert like) AGN at  $z=1.5-2.5$  higher

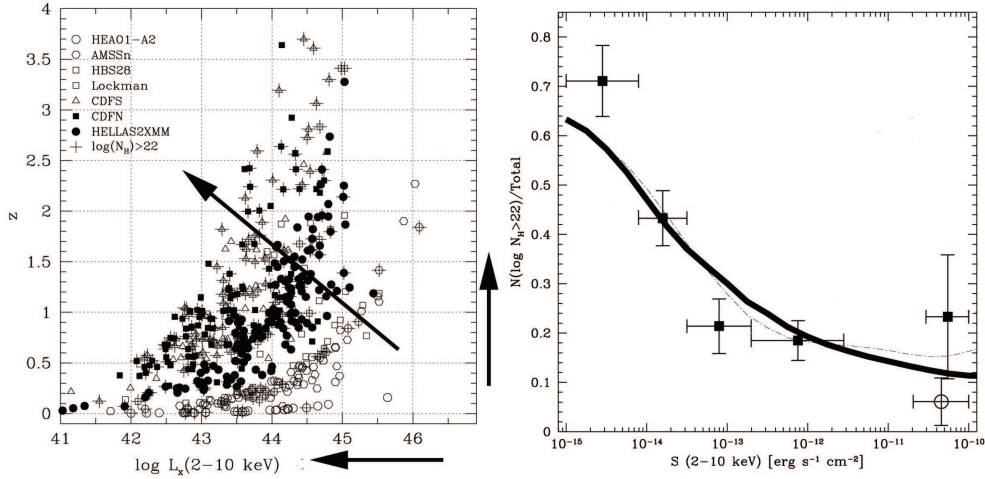


**Fig. 5.** Left panel: the luminosity-redshift plane for the surveys in Table 1. Crosses indicate AGN with  $N_H > 10^{22} \text{ cm}^{-2}$ . The arrows indicate the directions in which the fraction of obscured AGN increases, according to figure 4. Right panel: observed fraction of X-ray obscured ( $N_H > 10^{22} \text{ cm}^{-2}$ ) AGN as a function of  $F(2-10\text{keV})$

than what is observed by a factor of a few. This disagreement can be due to at least two broad reasons: either La Franca et al. (2005) underestimate the number of highly obscured AGN missed at  $z=1.5-2.5$  in Chandra and XMM-Newton surveys, or there are problems with the model.

About the first possibility, it must be noted that most obscured AGN selected below 10 keV have column densities in the range  $N_H \sim 10^{22-23} \text{ cm}^{-2}$  with only a handful of the faintest sources which may be Compton thick ( $N_H > 10^{24} \text{ cm}^{-2}$ , just  $\sim 4\%$  in the CDFS, Tozzi et al. 2006). So we still may be viewing just the tip of the iceberg of highly obscured sources. Our estimates of the number of obscured AGN missed in today X-ray surveys are based on large extrapolations from what we know about the fraction of obscured AGN in the local Universe. Compton thick objects may well be more common at high redshift, as suggested, for example, by Fabian (1999) and Silk & Rees (1998). An alternative approach to find Compton thick AGN at  $z > 1$  is to select sources with AGN luminosities in the mid-infrared and faint near-infrared and optical emission (Martinez-Sansigre et al.

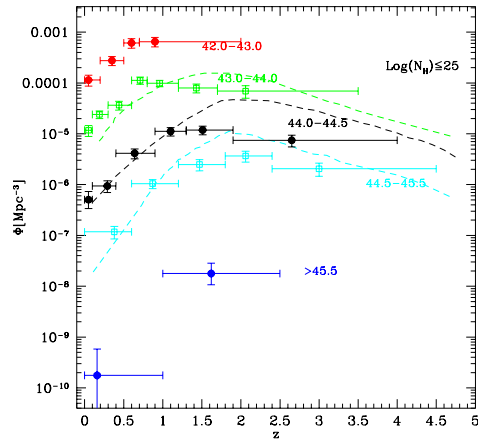


**Fig. 6.** The evolution of the number density of AGNs selected in the 2-10 keV band in three bins of luminosity ( $43 < \log L_X < 44$ ,  $44 < \log L_X < 44.5$ ,  $44.5 < \log L_X$ ) compared to the prediction of the model of Menci et al. (2004)

2005). These authors estimate that probably more than half of high luminosity QSOs are highly obscured, although with quite large uncertainties. Unfortunately, the X-ray proper-

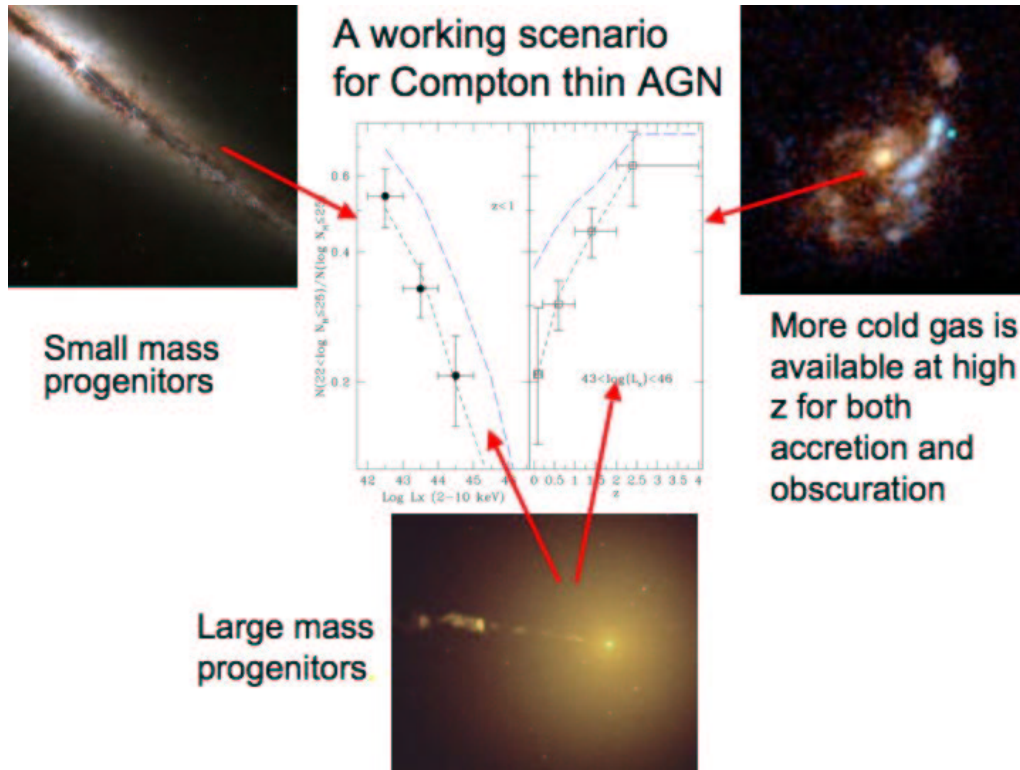


**Fig. 7.** A working scenario for Compton thin AGN

ties of these infrared selected sources are not known, and therefore it is difficult to understand how the mid-infrared selection compares with the X-ray one. In particular, it is not clear which is the fraction of the mid-infrared selected type 2 AGN which would have been selected by X-ray surveys. Answers to these questions will soon come from the study of fields with both X-ray and mid-infrared coverage (e.g. the ELAIS-S1 field, Puccetti et al. 2006, Feruglio et al. 2006 in preparation, and the COSMOS fields), and from deep X-ray follow-up observations of the mid-infrared selected sources in the Spitzer First Look Survey.

To avoid any possible selection effect, for an unbiased census of the AGN population making the bulk of the CXB and an unbiased measure of the AGN luminosity function at  $z=1-2$ , sensitive observations extending at the peak of the CXB are clearly needed. More specifically to resolve  $\sim 50\%$  of the

CXB in the 20–40 keV band we need to go down to fluxes of  $10^{-14}$  erg cm $^{-2}$  s $^{-1}$  in this band. This can be achieved only by imaging X-ray telescopes, (see e.g. Fiore et al. 2004, Ferrando et al. 2005). Key issues are: a) high collecting area; b) sharp PSF (15 arcsec or less Half Energy Diameter); c) low detector internal background.

About models, as in all complex processes, there are several areas which may be critical. For example, the prescriptions adopted by the Menci model to switch an AGN on and to compute its feedback on the host galaxy may be too simple, or, more in general, the descriptions of the mechanisms regulating the amount of cool gas in low-mass host galaxies and the physical mechanism at work at small accretion rates may be inadequate, as well as the statistics of DM condensations. Further constraints to this model, which may shed light on these issues, come from the observed correlations be-

tween the fraction of obscured AGN with luminosity and redshift. These correlations are at odds with popular AGN unified Schemes, and may suggest that low luminosity, Seyfert like AGN and powerful QSOs are intrinsically different populations, with different obscuration properties, caused by different formation histories, a bimodal behaviors reminding that of the color distribution of galaxies (see e.g. Menci et al. 2005). The Seyfer-like object population could be due to nuclear activation during loose galaxy encounters (fly-by, Cavaliere & Vittorini 2000) at sub Eddington levels, and the second population could be due to nuclear activation during major mergers, in the process of galaxy assembly. Seyfert like AGN could be mostly associated to galaxies with merging histories characterized by small mass progenitors while QSOs may be associated to large mass progenitors, as sketched in the cartoon of figure 7. In the first case nuclear accretion and star-formation could be self-regulated by feedbacks, which can therefore be effective in leaving available cold gas that can both cause an obscuration of the nucleus and be accreted during subsequent galaxy encounters. In these galaxies gas and dust lanes can efficiently obscure the nucleus along many lines of sight (a scenario similar to that outlined by Matt 2000). In the second case case feedback could be less effective in reheating/expelling the cold gas, most of which is rapidly converted in stars at high  $z$ . The obscuration properties of the two populations could be different in terms of gas geometry, covering factor, density, ionization state, metallicity, dust content and composition. A quantitative comparison between the prediction of the Menci model about the fraction of obscured AGNs with the observation is in progress. This comparison can help in both understanding which is the leading physical mechanism responsible for the activation and obscuration of AGNs of different luminosities, and in understanding the role of relative feedbacks between nuclear activity, star formation and galaxy evolution, as a function of the host mass and luminosity.

*Acknowledgements.* The original matter presented in this paper is the result of the effort of a large number of people, in particular of the HELLAS2XMM

collaboration: A. Baldi, M. Brusa, N. Carangelo, P. Ciliegi, F. Cocchia, A. Comastri, V. D’Elia, C. Feruglio, F. La Franca, R. Maiolino, G. Matt, M. Mignoli, S. Molendi, G. C. Perola, S. Puccetti N. Sacchi, and C. Vignali. I wish also to thank M. Elvis, P. Severgnini, N. Menci, A. Cavaliere, R. Gilli, G. Pareschi and O. Citterio. This work was partially supported by the Italian Space Agency (ASI) under grant I/023/05, by INAF under grant # 270/2003 and MIUR grant Cofin–03–02–23.

## References

- Akiyama, M., et al. 2000, ApJ, 532, 700  
 Barger, A.J., Cowie, L.L., Mushotzky, R.F. et al. 2005, AJ, 129, 578  
 Brandt, W.N., et al. 2001 AJ, 122, 2810  
 Cavaliere, A. & Vittorini, V 2000, ApJ, 543, 599  
 Cocchia, F., Fiore, F., Mignoli, M. et al. 2006, A&ASubmitted  
 Comastri, A., Fiore, F., Vignali, C. et al. 2001, MNRAS, 327, 781  
 Comastri, A., Mignoli, M., Ciliegi, P. et al. 2002, ApJ, 571, 771  
 Cowie L., Barger A., Bautz, M.W., Brandt, W.N., & Garnire, G.P. 2003, ApJ, 584, L57  
 Fabian, A.C. 1999, MNRAS, 308, L39  
 Ferrarese, L., & Merrit, D., 2000, ApJ, 539, L9  
 Fiore, F., La Franca, F., Giommi, P., Elvis, M., Matt, G., Comastri, A., Molendi, S., & Gioia, I. 1999, MNRAS, 306, L55  
 Fiore, F., La Franca, F., Vignali, C. et al. 2000, NewA, 5, 143  
 Fiore, F., Brusa, M., Cocchia, F., et al. 2003, A&A, 409, 79  
 Fiore, F., Perola, G.C., Pareschi, G., Citterio, O., Anselmi, A. & Comastri, A. 2004, Proceedings of SPIE Vol. 5488, “UV to Gamma Ray Space Telescope Systems”, astro-ph/0407647  
 Ferrando, P. et al. 2005, Proc. of SPIE conference “Optics for EUV, X-Ray, and Gamma-Ray Astronomy II”, astro-ph/0508674  
 Franceschini, A., Hasinger, G., Miyaji, T., & Malquori, D., 1999, MNRAS, 310, L5  
 Gebhardt, K., Kormendy, J., Ho, L., et al. 2000, ApJ, 543, L5  
 Giacconi, R., et al. 2002, ApJS, 139, 369  
 Hasinger, G., 2003, in “The Emergence of Cosmic Structure”, Maryland, eds.

- Stephen S. Holt and Chris Reynolds, astro-ph/0302574
- Hasinger, G., Miyaji, T. & Schmidt M. 2005, A&A, 441, 417
- Koekemoer et al. 2004, ApJL, 600, L123
- La Franca, F., Fiore, F., Vignali C. et al. 2002, ApJ, 570, 100
- La Franca, F., Fiore, F., Comastri, A. et al. 2005, ApJ, 635, 864
- Lawrence, A. & Elvis, M. 1982, ApJ, 256, 410
- Miyaji, T., Hasinger, G. & Schmidt, M. 2000, A&A, 353, 25
- Maiolino, R., Mignoli, M., Pozzetti, L. et al. 2006, A&A, 445, 457
- Marconi, A. & Hunt, L. 2003
- Marconi, A., Risaliti, G., Gilli, R., Hunt, L. K., Maiolino, R. & Salvati, M. 2004, MNRAS, 351, 169
- Matt, G. 2000, A&A, 355, L31
- Martinez-Sansigre, A., Rawlings, S., Lacy, M. et al. 2005, Nature, 436, 666
- Mignoli, M., Pozzetti, L., Comastri, A. et al. 2004, A&A, 418, 827
- Menci, N., Fiore, F., Perola, G.C., & Cavaliere, A. 2004, ApJ, 606, 58
- Menci, N., Fontana, A., Giallongo, E. & Salimbeni, S. 2005 ApJ, 632, 49
- Perola, G. C, Puccetti, S., Fiore, F. et al. 2004, A&A, 421, 491
- Piconcelli, E., Cappi, M., Bassani, L., Di Cocco, G. & Dadina, M. 2003, A&A, 412, 689
- Puccetti, S., Fiore, F., D'Elia, V. et al. 2006, A&A, in press
- Silk, J. & Rees, M.J. 1998, A&A311, L1
- Tozzi, P., Gilli R. Mainieri V. et al. 2006, ApJin press, astro-ph/0602127
- Ueda, Y., Akiyama, M., Ohta, K., & Miyaji, T., 2003, ApJ, 598, 886